AGU PUBLICATIONS

JGR

Journal of Geophysical Research: Atmospheres

RESEARCH ARTICLE
10.1002/2016JD026409

Key Points:
- The recirculation phenomenon is well studied using computer simulations and wind tunnel experiments but has not been examined thoroughly in the atmosphere over complex terrain
- The primary causes of recirculation in the atmosphere are the wake effect of an obstruction combined with a negative vertical potential temperature gradient
- Recirculation changes the CO_2 concentration measured above forest canopies due to vertical mixing and also influences the energy flux and CO_2 flux measured using the eddy covariance method

Correspondence to:
C. Yi,
cyi@qc.cuny.edu

Citation:
Kutter, E., C. Yi, G. Hendrey, H. Liu, T. Eaton, and W. Ni-Meister (2017), Recirculation over complex terrain, *J. Geophys. Res. Atmos.*, *122*, doi:10.1002/2016JD026409.

Received 22 DEC 2016
Accepted 17 MAY 2017
Accepted article online 22 MAY 2017

Recirculation over complex terrain

Eric Kutter[1,2], Chuixiang Yi[1,2], George Hendrey[1,2], Heping Liu[3], Timothy Eaton[2], and Wenge Ni-Meister[4]

[1]Earth and Environmental Sciences Department, Graduate Center, City University of New York, New York, New York, USA, [2]School of Earth and Environmental Sciences, Queens College, City University of New York, New York, New York, USA, [3]Department of Civil and Environmental Engineering, Washington State University, Pullman, Washington, USA, [4]Department of Geography, Hunter College of the City University of New York, New York, New York, USA

Abstract This study generated eddy covariance data to investigate atmospheric dynamics leeward of a small, forested hillside in upstate New York. The causes and effects of recirculation eddies were examined to support the larger goal of improving measurement of the exchange of energy, moisture, and trace gases between the terrestrial biosphere and the atmosphere over complex terrain. Sensors operated at five different altitudes on two separate towers—one at the top of the hill and one down the slope to the east—for approximately 8 weeks in the spring of 2013. During the experiment, the vertical potential temperature gradient was found to be the primary factor for determining whether winds interacting with the terrain features caused a recirculating eddy leeward of the hill. The study found evidence that the recirculation influenced carbon dioxide flux and caused the air column to be vertically well mixed.

Plain Language Summary The purpose of our overall research project is to improve our understanding of biosphere/atmosphere interactions in nonhomogeneous natural environments. We used the eddy covariance method, which, while imperfect, has been instrumental in furthering knowledge of boundary layer interactions. Seeking additional improvements to such a powerful tool is a worthwhile endeavor, and we hope to advance the technique as we pursue the main project goal. Previous studies in this field have focused on the energy flux balance closure problem, where net radiation measurements often record larger-energy flux than researchers can account for within their observed systems. Eminent scientists have predicted various causes of this imbalance: advection, energy storage, etc. Many proposed "errors" fall into the category of nonturbulent fluxes. We postulate that a large, slow-moving recirculation bubble spinning leeward of a forested hillside may cause a significant amount of flux and other boundary layer changes that would not be captured using the standard eddy covariance method. We know these recirculation bubbles occur due to work by other scientists in hydraulics observations, or through atmospheric modeling. Our two towers were designed to capture this recirculation effect, identify its causes, and begin the process of understanding its impacts.

1. Introduction

A recirculation zone is a vortex with a horizontal axis, occurring downstream of a fluid flowing past an obstruction [*Whiteman*, 2000]. While recirculation commonly occurs after an abrupt change in topography the phenomenon can also be caused by gentle slopes under certain atmospheric conditions [*Xu and Yi*, 2012]. Recirculation is generally associated with vertical shear and increased turbulence in the fluid [*Stull*, 1988]. Considering the atmosphere leeward of a forested hillside, recirculating air may theoretically reach from the forest floor up to an altitude above the hilltop [*Stull*, 1988]. This air circulation influences vertical mixing of energy and trace gases [*Staebler and Fitzjarrald*, 2005; *Xu and Yi*, 2012] and the direction and magnitude of fluxes [*Raupach and Thom*, 1981; *Feigenwinter et al.*, 2010].

Wind tunnel and numerical model simulations combined with observations in the hydraulics field have shown recirculation eddies appearing leeward of an obstruction [*Poggi and Katul*, 2007; *Wang and Yi*, 2012], causing significant impacts on the distribution of trace gas pollutants [*Dawson et al.*, 1991]. Numerical simulations that focused on the wind dynamics around hills found evidence of recirculation, with potential effects on CO_2 concentration and CO_2 flux [e.g., *Katul et al.*, 2006; *Xu et al.*, 2015, 2017]. Recirculation (reversed flow) within the canopy on the hill slope was predicted by a numerical model around a hill in a thermally neutral atmosphere [*Finnigan and Belcher*, 2004], for a critical value of canopy thickness. Updating that model, expanded predictions of recirculation were made over more complex terrain

[*Wang and Yi*, 2012]. Other studies have shown wind interactions with complex terrain features producing lee waves without recirculation [*Wurtele et al*., 1993]. However, the influence of recirculation on flux near the ground surface, and ultimately on net ecosystem exchange, has not been thoroughly examined in situ. The primary goal of the study focuses on understanding what atmospheric conditions cause recirculation eddies instead of lee waves with no recirculation, what strengthens or weakens the phenomenon, and what impacts recirculation may have on concentration profiles and fluxes. An experiment was conducted using two eddy flux towers with sensors at multiple heights at each tower.

Throughout the experiment, we used the eddy covariance method to measure energy and trace gas flux using the standard assumptions as described by *Baldocchi et al.* [1988]. These assumptions are most appropriate when the observations occurred over horizontally level ground, with homogeneous vegetation and other land features, without any sources or sinks above the surface. Such unrealistic assumptions are a major drawback to using the eddy covariance method in most areas of the terrestrial ecosystem with more complex vegetation and topography. Since these assumptions differ from conditions at our site and most eddy flux tower sites, calculated fluxes are bound to contain errors due to the complex terrain [*Baldocchi*, 2003]. Many researchers have attempted to reduce or eliminate those errors by using varying combinations of theoretical methods, computer simulations, and/or physical observations [e.g., *Goulden et al*., 1996; *Foken*, 2008; *Finnigan*, 2008].

Of the many potential sources of error in the eddy covariance method that were discovered during those attempts, several point to recirculation as a probable culprit. In some locations, large-scale, slow-moving eddies with a frequency of less than 0.1 Hz dominated the total measured flux [*Goulden et al*., 1996]. It has been reported that sites in hilly or forested land have complex interactions with their topographies and canopy structures leading to eddies that are stable and predictable [*Finnigan*, 2008; *Foken*, 2008]. A recirculation vortex is a large-scale, eddy structure caused by interactions between a fluid and an obstruction, or in other words, the synoptic wind and complex terrain. Our theory envisions recirculation as a vertical mixing phenomenon molded into a persistent shape by the geometry of the topography interacting with the synoptic wind direction. This study focused on a forested hillside with the purpose of observing these complex interactions, and then predicting when recirculation would form in the lee of the hill.

Since imprecise accounting for fluxes caused by recirculation vortices (large-scale eddy structures) using eddy covariance data processing methods explains a part of the energy flux imbalance [*Foken*, 2008], understanding the causes and impacts of recirculation is one necessary step toward correcting the energy flux imbalance problem and improving eddy covariance over complex terrain.

Understanding the exchange of energy, moisture, and trace gases between the terrestrial biosphere and the atmosphere over complex terrain is a fundamental goal in achieving a complete model of global or regional climate. Net ecosystem exchange (NEE) of carbon dioxide is often a crucial input into climate models or is used as a means of validating regional model outputs [e.g., *Papale and Valentini*, 2003]. Calculations obtained from eddy flux tower data provide some of the best quality sources of NEE values, typically using friction velocity as an indicator of data quality. However, the standard formulation of the eddy covariance method assumes steady state flow, zero advection both vertically and horizontally, and no air flow divergence or convergence. A recirculation vortex violates those assumptions, partially undermining confidence in tower-based eddy flux data over complex terrain. The following field observation of atmospheric dynamics over complex terrain was designed to identify the causes and some effects of recirculation as a means of closing part of the existing knowledge gap.

2. Method

Two eddy flux towers were set up on a forested hillside in Black Rock Forest (BRF), New York (Figure 1), to collect measurements of atmospheric dynamics from 21 April to 9 June 2013. The towers were aligned in the east-west direction since historical wind data around the hillside showed prevailing wind from the west (BRF Consortium, personal communication about unpublished data). The towers were designed to carry instrumentation to identify and then examine the recirculation (stable and predictable low-frequency eddy structures) mentioned above.

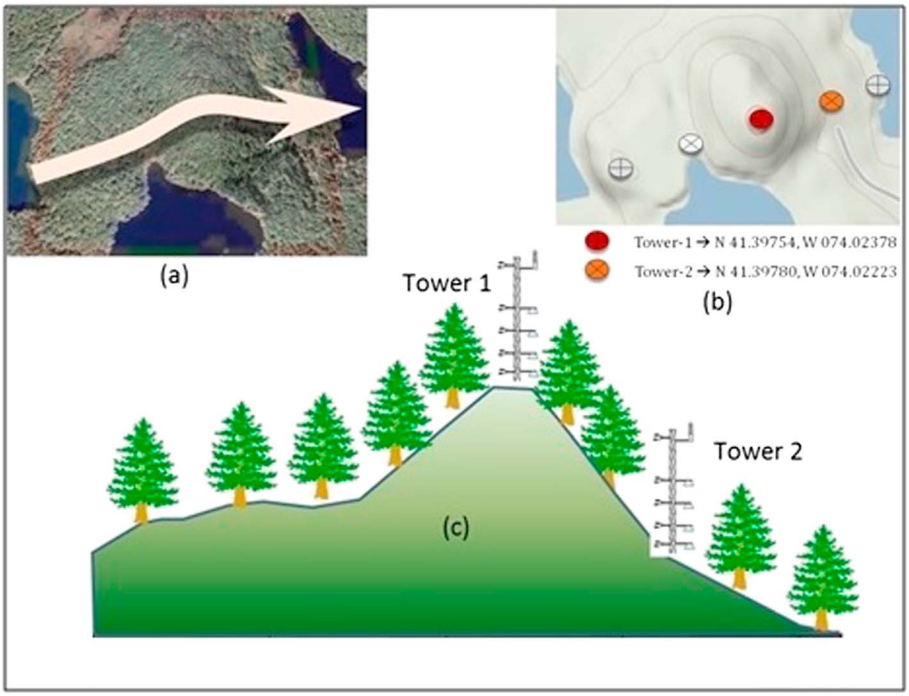

Figure 1. A schematic of the tower installation: (a) An aerial view of the location, with the dominant westerly winds indicated. (b) Locations of the two towers and their geographic coordinates (the white circles are locations for a planned expansion). (c) Rough sketch of the two towers and their heights compared with the average canopy height. The slope is exaggerated in Figure 1c: the vertical scale and horizontal scales are different.

The two-tower system collected eddy covariance measurements both within and above the canopy. Tower 1 was located at the top of the hill, which rises roughly 40 m above the surrounding area. Tower 2 was slightly below midslope of the same hill, approximately 130 m east of Tower 1. The average slope of the hill between the towers was 20% (about 11°). The forest was mixed, including both conifer and deciduous trees at an average maximum height of 14 m near the towers, with significant underbrush. The canopy depth was 9 to 10 m at each tower, which was well in excess of the minimum 1.7 m canopy depth predicted to be required to cause recirculation [*Finnigan and Belcher*, 2004]. A small lake was located approximately 200 m farther east of Tower 2.

Open-path infrared gas analyzers (IRGAs) and 3-D sonic anemometers were placed at five levels on Tower 2, plus the top level of Tower 1, to collect data at 10 Hz. The remaining four levels of Tower 1 used 2-D sonic anemometers and a closed-path IRGA with a manifold system allowing it to sample all four levels in sequence. The lower four levels of Tower 1 sampled data at a low frequency of 1 Hz or 1/3 Hz, depending on the sensor. Temperature sensors were located at all five levels of each tower. The top level of each tower also had a net radiometer, a photosynthetically active radiation (PAR) meter, and additional sensors measuring temperature, humidity, and atmospheric pressure. The top level of Tower 2 had a basic albedo determination comprising two opposite-facing photometers. The bottom three levels of Tower 2 had additional PAR meters installed. Soil moisture and ground heat flux probes were used to measure the terrestrial dynamics near each tower. Both towers took measurements at 2, 5, 8, 14, and 26 m above the respective tower's base. The full suites of sensors installed on and around Towers 1 and 2 are shown in Figures 2a and 2b, respectively.

The data were captured using a combination of CR1000 and CR5000 data loggers. The entire system was powered using marine batteries charged by a small gasoline-powered generator serving each tower. The generators were each located more than 100 m north of their respective towers in order to minimize or eliminate carbon dioxide and heat contamination of the data.

Instruments were calibrated in the laboratory prior to installation. IRGAs were tested using compressed gas cylinders and a dewpoint generator. At the end of the project, all IRGAs were re-examined in the lab using

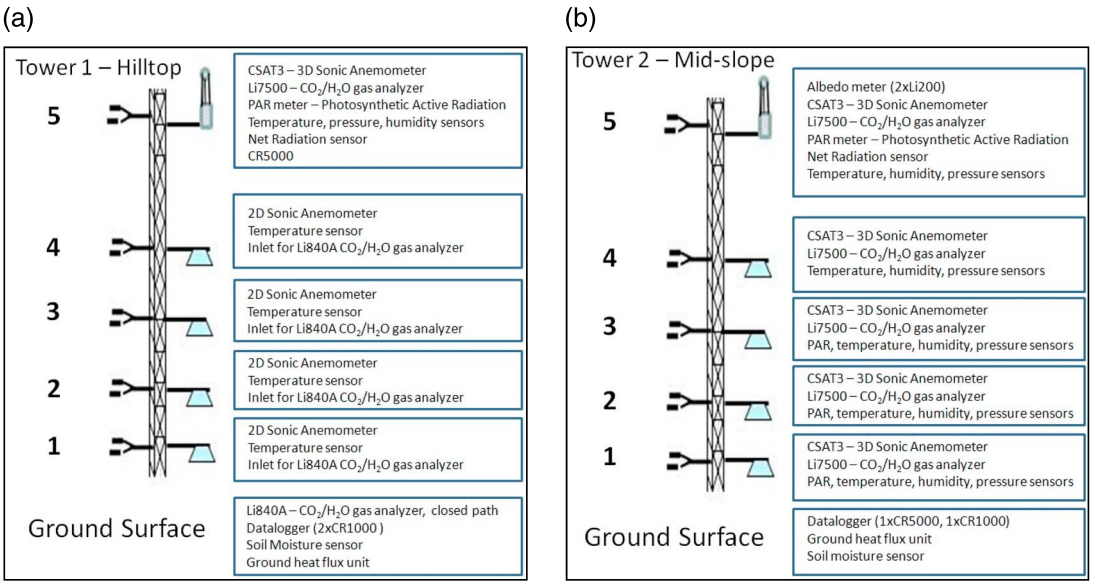

Figure 2. (a) Schematic showing sensor installations at each level of Tower 1, the hilltop tower. Note that the top level contains the high-frequency sensors associated with the eddy covariance technique, while supporting measurements are taken at the within-canopy levels. (b) This schematic shows the composition of all sensors installed at Tower 2, on the slope of the hillside. All levels contain the typical eddy flux sensor suite. Some levels are also equipped with additional supporting sensors designed to supplement the eddy flux measurements.

the same cylinders and dewpoint generator. The reanalysis confirmed no significant instrumental drift had taken place during the relatively brief observation period.

The collected 10 Hz data were initially processed using Eddy Pro® software (version 5.2.1) according to the methods in *Burba and Anderson* [2010]. We used the planar fit method of coordinate rotation [*Wilczak et al*., 2001] over the entire project period, discarding wind flows from within the wind shadow of the towers, as well as the Webb, Pearman, and Leuning method of correcting for the effects of air density [*Webb et al*., 1980].

In terms of processing quality control, we used a Hamming tapering window prior to the fast Fourier transform of the time series, as suggested by *Kaimal and Kristensen* [1991]. Footprint estimations were made according to *Kljun et al.* [2004], and the data were evaluated using the policies in *Mauder and Foken* [2004]. High-pass filtering effects were corrected as set forth by *Moncrieff et al.* [2004], while the low-pass filtering effect corrections were conducted according to *Moncrieff et al.* [1997]. The raw data were also checked for spikes, amplitude variance compared with instrument sensitivity, dropouts, absolute limits (to ensure that all measured parameters were physically possible), skewness, and kurtosis prior to data processing as specified by *Vickers and Mahrt* [1997]. The low-frequency data were converted manually into 30 min averages that matched the time periods of the processed eddy covariance data.

To identify the wave conditions in the lee of the hill, we calculated the Brunt-Väisälä frequency (adapted from *Stull* [1988]) using

$$f = \frac{\sqrt{\left(-\frac{g}{\theta} * \frac{\mathrm{d}\theta}{\mathrm{d}z}\right)}}{2\pi} \tag{1}$$

with acceleration due to gravity (g) at -9.8 m s^{-2}; the potential temperature (θ) calculated from the sonic temperature, or from fine-wire thermocouples for those levels that did not have 3-D sonic anemometers; and the gradient of potential temperature with height (dθ/dz) estimated using the sonic temperatures measured at the top two levels at Tower 2.

Gu et al. [1999] modified the procedure set forth by *Budyko* [1958] to determine the degree of error in energy flux measurements in terms of an energy flux balance ratio (EBR):

$$\mathrm{EBR} = \frac{\lambda E + FH}{R_n - G} \tag{2}$$

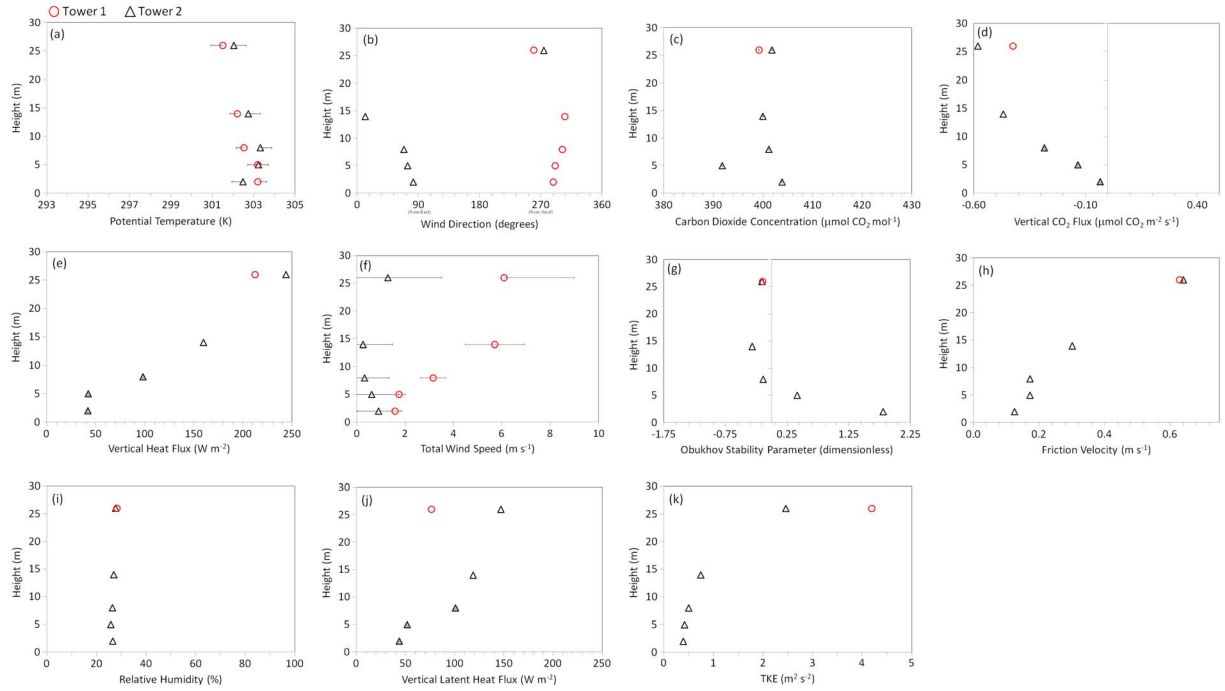

Figure 3. Charts of the observation results at 2:30 P.M. on 16 May 2013, showing (a) potential temperature, (b) wind direction, (c) carbon dioxide concentration, (d) carbon dioxide flux, (e) heat flux, and (f) total wind speed. Tower 1 results are represented by red circles; while Tower 2 data are black triangles. Gray triangles indicate fluxes with $u_* < 0.17$ m s^{-1}. Charts of the observation results at 2:30 P.M. on 16 May 2013, showing (g) Obukhov stability parameter, (h) friction velocity, (i) relative humidity, (j) vertical latent heat flux, and (k) turbulent kinetic energy. Tower 1 results are represented by red circles, while Tower 2 data are black triangles. Gray triangles indicate fluxes with $u_* < 0.17$ m s^{-1}.

where R_n is the net radiation, G is ground heat flux, F_H is sensible heat flux, and λE is latent heat flux. To avoid introducing bias through gap-filling of missing data points [*Baldocchi*, 2003], EBR was calculated using only those 24 h periods (defined as the 30 min averages from 5:30 P.M. to 5:00 P.M. the next day) where complete or nearly complete records were available, missing no more than two (2) 30 min averages. Any missing parameters within any 30 min time period caused the rejection of that 30 min period from the 24 h EBR calculation. Given those criteria, we used 27 daily records at Towers 1 and 19 at Tower 2 (not necessarily the same days) to generate our total project EBR. The calculations resulted in an EBR of approximately 80% at Tower 1 and 86% at Tower 2. This degree of energy flux balance error is not unusual for FLUXNET locations above canopies in complex terrain [*Wilson et al*., 2002].

In section 3 below, note that total wind speed measured at the bottom four levels of Tower 1 were measured with two-dimensional sonic anemometers, not the 3-D sonic anemometers that recorded wind speeds at the top level of Tower 1 and at all levels of Tower 2. Where possible, error bars for key parameters were established using one sample standard deviation over the 30 min average in question. Since wind direction variability was not provided by the EddyPro® software, wind roses presented in the results section were generated by hand using the raw, high-frequency data. The time periods discussed in section 3 below have friction velocities above the minimum 0.17 m s^{-1} threshold [*Goulden et al*., 1996] at least at the top level both towers and often for multiple levels within the forest canopy at Tower 2 (see Figures 3h, 5h, 6h, and 7h).

3. Results and Discussion

During the experiment, the aerodynamic profile around the hillside was primarily controlled by the wind direction and by the atmospheric stability in terms of the vertical potential temperature gradient. Whenever synoptic conditions caused the background wind direction to be westerly, our two-tower system recorded one of three different atmospheric patterns. We will analyze examples of the three cases and then discuss the single time period when the vertical potential temperature gradient failed to predict atmospheric dynamics leeward of the hillside.

Table 1. Frequency of Conditions Represented by Three Example Cases

Thermal Stability	Occurrences in Days (Instances)	Recirculation Occurrences	Average Duration (h)
Unstable	12 (19)	19 full	3.2
Near Neutral	11 (13)	13 partial	2.0
Stable	7 (11)	1 partial	3.3

The project site experienced westerly or near westerly winds with both towers functioning on 15 different days, often with multiple different states and separate instances of one or more states during each day. While it is difficult to determine with certainty the exact time the atmosphere turned thermally unstable—or a recirculation vortex formed or dissipated—using real-world observations averaged into 30 min time periods, Table 1 summarizes our best estimates of the results obtained. The table uses time periods when most of the Tower 1 wind results were within 45° of westerly. A weak thermal stability or instability did not influence the atmospheric flow at the project site, leading to a distinction between the accepted definition of neutral conditions (i.e., 1°C per 100 m) and this paper's usage of the term

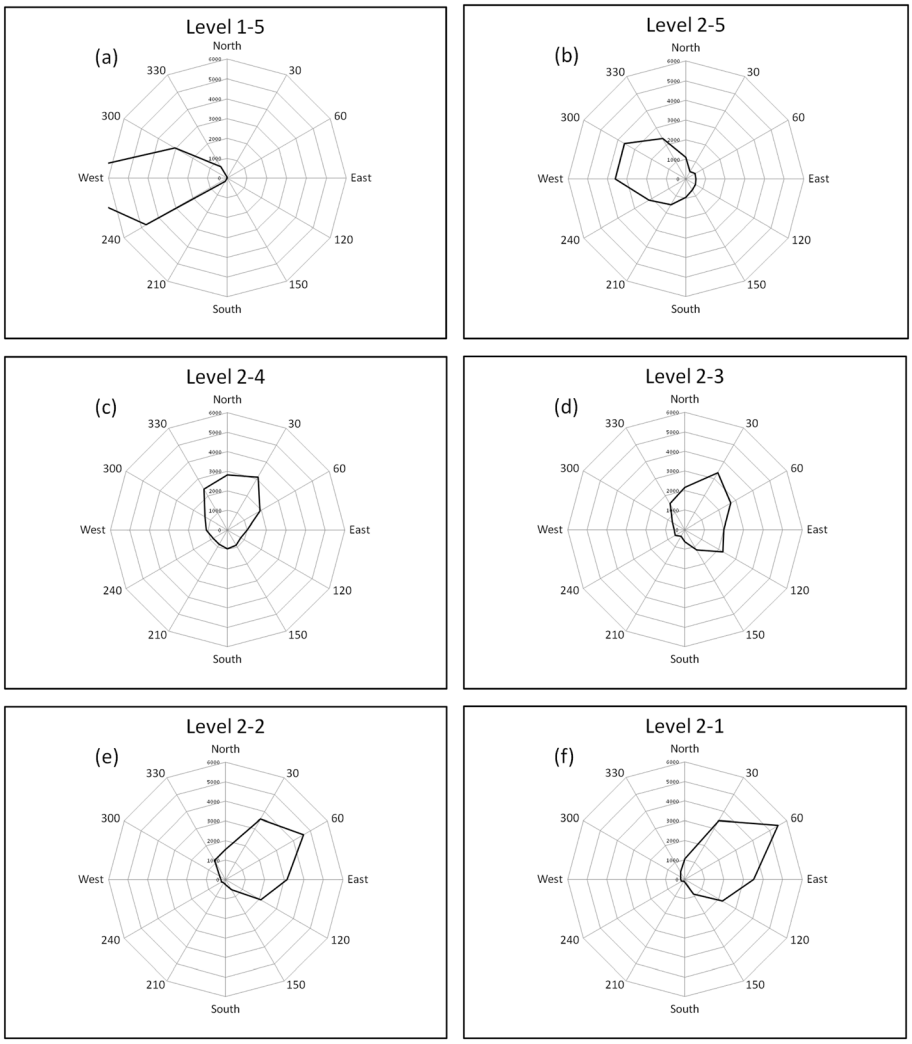

Figure 4. Wind roses (in degrees) at 2:30 P.M. on 16 May 2013, showing (a) top of Tower 1, (b) top of Tower 2, (c) top of canopy at Tower 2, (d) midcanopy at Tower 2, (e) lower canopy at Tower 2, and (f) trunk space at Tower 2. The wind roses were assembled using counts of the unrotated wind direction collected at 10 Hz over 30 min and are not weighted by wind speed.

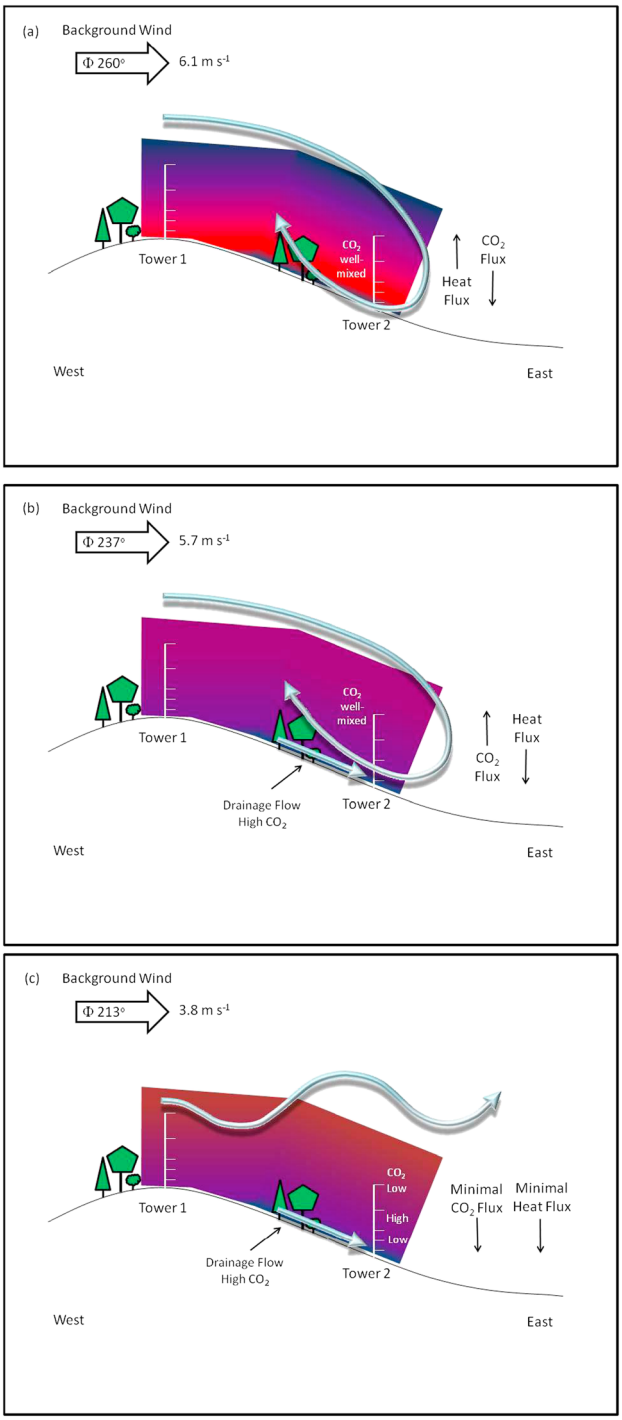

Figure 5. Conceptual two-dimensional sketches of wind dynamics around the experiment in various atmospheric conditions. The red coloring indicates warmer air, while the darker blues and purples represent colder air. (a) Recirculating air reaching the ground on the slope during this time period. (b) We note nearly uniform potential temperature, with a very slight warming near the top of Tower 1. Recirculating air did not reach the ground on the slope during this time period, instead changing to katabatic drainage flow near the forest floor around Tower 2. (c) Slightly warmer air aloft. Recirculation was not evident during this time period. Note also that carbon dioxide flux is negative (downward) at most levels during this time, which is unexpected during nighttime.

"near neutral." During the project, near neutral atmospheric condition refers to a lapse rate (positive or negative) from the midcanopy to the top of the tower below 2°C per 100 m. The trunk space is ignored for that determination since the near-ground temperature did not appear to influence the presence, absence, or extent of recirculation during any time period.

3.1. Case 1—Unstable Atmosphere

At 2:30 P.M. on 16 May 2013, the vertical potential temperature profile at Tower 1 showed warm air close to the ground, with colder air aloft. A similar pattern was observed at Tower 2, except for slightly colder air at the very bottom of the slope tower. This profile was unstable at the hilltop and unstable on the slope generally, with the near-ground air under stable conditions on the slope (Figure 3a). The wind directions at all levels of Tower 1 were westerly. Tower 2 recorded a westerly wind at the top level above the canopy, while within the canopy the winds were generally easterly (northerly at the very top of the canopy) (Figure 3b). Wind roses provide an additional visual indication of wind direction and its variability (Figures 4a–4f). This wind pattern is indicative of recirculation reaching the forest floor. *Finnigan and Belcher* [2004, Figure 4] predicted a somewhat similar pattern under neutral atmospheric conditions (they did not present findings in an unstable atmosphere). A conceptual sketch of the hillside air dynamics for Case 1 is included as Figure 5a. Due to the negative gradient of the potential temperature with height, the Brunt-Väisälä frequency was a nonzero complex number. Since in general a complex solution to an eigenvalue frequency equation presents in its phase space as a focus spiraling into a point or a source spiraling outward, the air parcel is expected to follow a spiral pattern, eventually forcing air to flow perpendicular to the plane of the experimental setup (in this case, to the north or south).

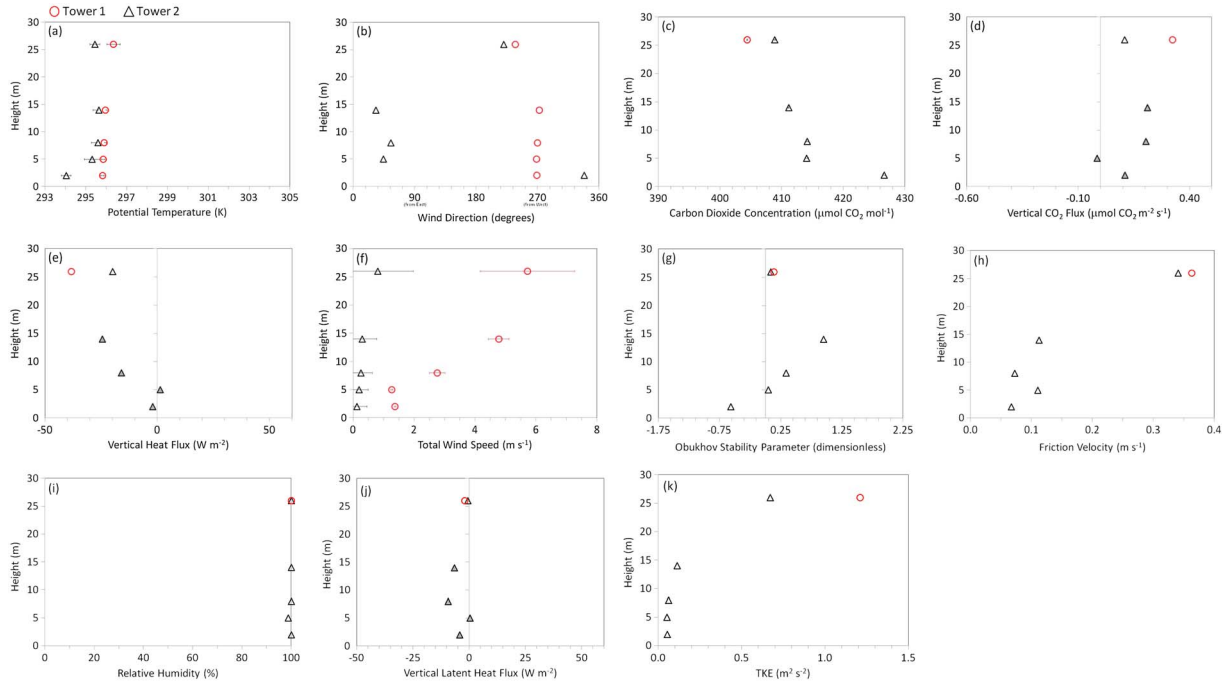

Figure 6. Charts of the observation results at 2:30 A.M. on 21 May 2013, showing (a) potential temperature, (b) wind direction, (c) carbon dioxide concentration, (d) carbon dioxide flux, (e) heat flux, and (f) total wind speed. Tower 1 results are represented by red circles, while Tower 2 data are black triangles. Gray triangles indicate fluxes with $u_* < 0.17$ m s^{-1}. Charts of the observation results at 2:30 A.M. on 21 May 2013, showing (g) Obukhov stability parameter, (h) friction velocity, (i) relative humidity, (j) vertical latent heat flux, and (k) turbulent kinetic energy. Tower 1 results are represented by red circles, while Tower 2 data are black triangles. Gray triangles indicate fluxes with $u_* < 0.17$ m s^{-1}.

Due to the recirculating air and the unstable atmosphere, carbon dioxide at Tower 2 was well mixed through both mechanical and thermal means (Figure 3c), with concentrations substantially similar at most levels of Tower 2. Vertical carbon dioxide flux at both towers was negative or downward (Figure 3d), and vertical sensible heat flux (hereafter referred to as "heat flux" unless otherwise specified) upward (Figure 3e), as expected during daytime in the growing season. The total wind speeds (Figure 3f) recorded increasing speed with height at Tower 1. However, the wind at Tower 2 was at a minimum in midcanopy where maximum leaf density was located [*Yi*, 2008], while the top level wind speed of 1.3 m s^{-1} was similar in magnitude to the speed in the trunk space, 0.90 m s^{-1}.

The Obukhov stability parameter [*Monin and Obukhov*, 1954] predicted an unstable atmosphere at the upper three levels of Tower 2, switching to stable in the bottom two levels (i.e., at 2 and 5 m above the ground—see Figure 3g). *Foken* [2006] argued that the Monin-Obukhov similarity theory is of limited usefulness over (or within) tall vegetation or on sloped terrain. In many other cases during our study, the Obukhov stability parameter did not provide reasonable predictions; however, for the time period of Case 1 the unstable atmosphere was closely predicted by the Obukhov stability parameter.

Relative humidity was roughly constant at all heights of Tower 2 (Figure 3i), ranging from 25.7% to 26.9% within canopy, and 28.2% above the forest. In the absence of an influx of moisture at the lower levels of Tower 2, we conclude that the recirculation region did not reach the lake on the valley floor to the east of Tower 2 during this time period, and therefore, the recirculation zone was similar in scale to the hill obstructing the synoptic air flow.

3.2. Case 2—Neutral Atmosphere

At 2:30 A.M. on 21 May 2013, both towers recorded vertical potential temperature gradients near zero, corresponding to near neutral atmospheric conditions (Figure 6a), except for slightly stable air at the top of Tower 1 and at the bottom level of Tower 2. The wind direction at the top of Tower 1 was southwesterly and westerly within the canopy. Tower 2 recorded wind (Figure 6b) from the southwest at the top level above the canopy, while within the canopy the winds were generally northeasterly. The wind was northerly near the ground level, apparently following the gentle gradient of the valley down toward the Hudson River in the

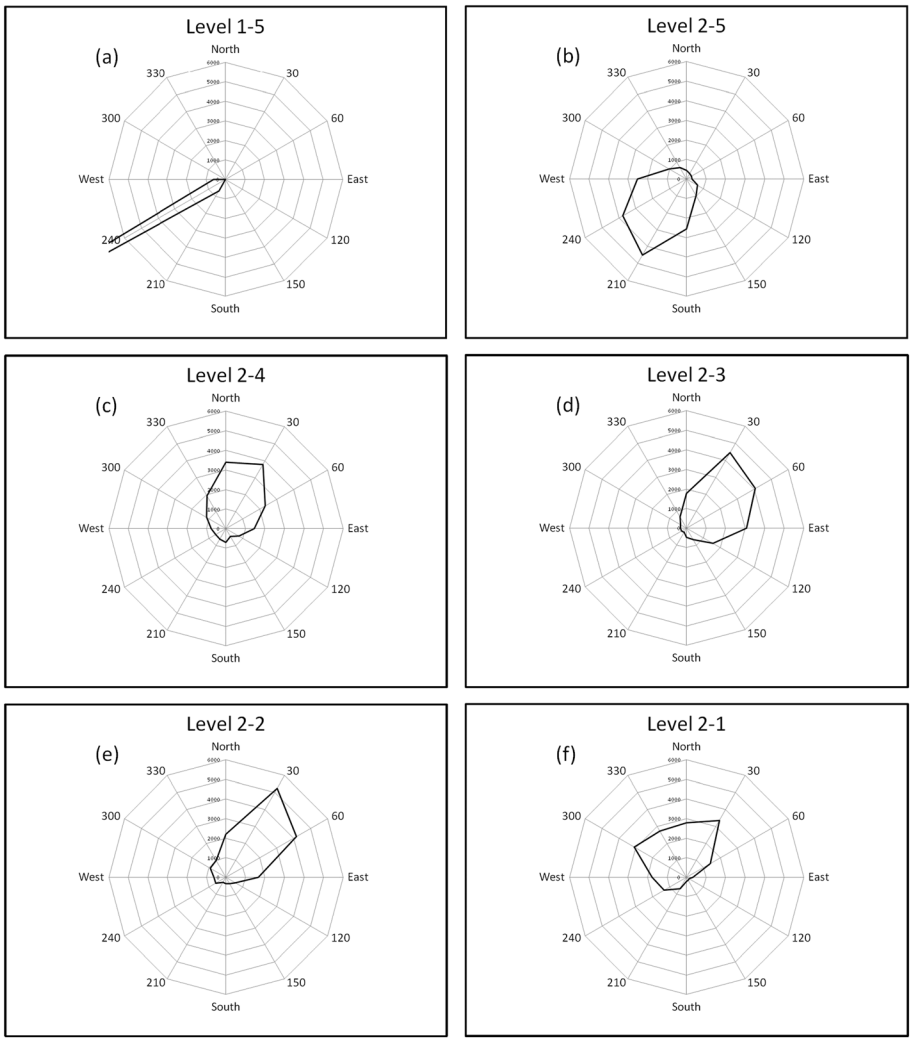

Figure 7. Wind roses (in degrees) at 2:30 A.M. on 21 May 2013, showing (a) top of Tower 1, (b) top of Tower 2, (c) top of canopy at Tower 2, (d) midcanopy at Tower 2, (e) lower canopy at Tower 2, and (f) trunk space at Tower 2. The wind roses were assembled using counts of the unrotated wind direction collected at 10 Hz over 30 min and are not weighted by wind speed.

south [*Tóta et al*., 2008]. Wind roses provide an additional visual indication of wind direction and its variability to mitigate possible inaccuracies in average wind direction during periods of low wind speed (Figures 7a–7f).

This wind pattern is indicative of a partial recirculation penetrating into the forest canopy but not reaching the ground level. A conceptual sketch of the hillside air dynamics for Case 2 is included as Figure 5b. Due to the nearly constant potential temperature with height, the Brunt-Väisälä frequency was approximately zero. As in Case 1, Tower 2 data showed no indication of lee waves above the recirculation.

Due to the incomplete recirculation, carbon dioxide at Tower 2 was somewhat mixed (Figure 6c), maintaining a slight negative gradient with height of about 5 ppm in 21 m, with high CO_2 concentrations near ground level where the recirculation pattern did not reach. If the recirculation had reached the CO_2-rich air at the forest floor, the CO_2 concentration at the top of Tower 2 (where flux towers most commonly take measurements) would be higher. CO_2 flux at both towers was mostly positive or upward (Figure 6d), with heat flux negative or downward (Figure 6e), as expected at night in the absence of photosynthesis. Both fluxes were nearly zero at the second level of Tower 2, indicating that the recirculation of air at Tower 2's location on the hillside reached down to a height near 5 m above the forest floor. A layer of air with no vertical carbon dioxide flux or heat flux then separated the recirculating upper air mass from the stable near-ground layer

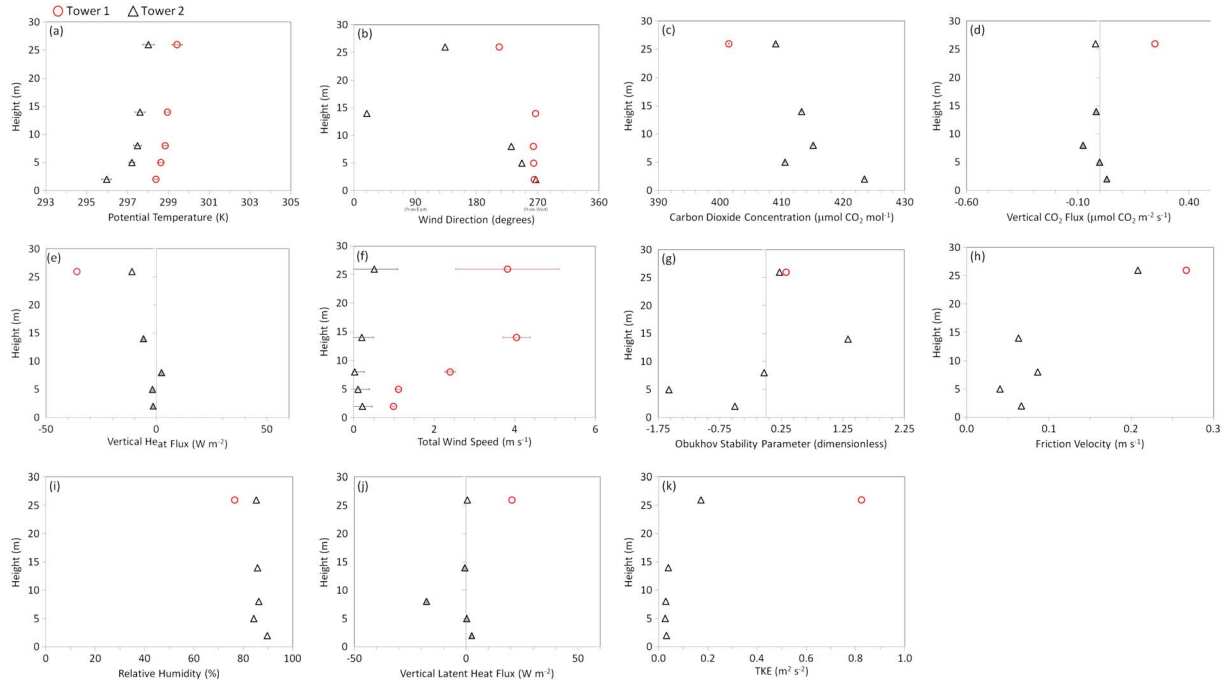

Figure 8. Charts of the observation results at 1:00 A.M. on 30 May 2013, showing (a) potential temperature, (b) wind direction, (c) carbon dioxide concentration, (d) carbon dioxide flux, (e) heat flux, and (f) total wind speed. Tower 1 results are represented by red circles, while Tower 2 data are black triangles. Gray triangles indicate fluxes with $u* < 0.17$ m s^{-1}. Charts of the observation results at 2:30 A.M. on 21 May 2013, showing (g) Obukhov stability parameter, (h) friction velocity, (i) relative humidity, (j) vertical latent heat flux, and (k) turbulent kinetic energy. Tower 1 results are represented by red circles, while Tower 2 data are black triangles. Gray triangles indicate fluxes with $u* < 0.17$ m s^{-1}.

subjected to katabatic flow (Figure 6b), draining cold air slowly downslope [*Yi et al.*, 2005; *Chen and Yi*, 2012] along the valley toward the lower elevation Hudson River to the south and east.

The total wind speeds increased with height at both towers (Figure 6f), but with a much higher gradient at Tower 1. The wind speed at Tower 2 did not have a midcanopy minimum caused by the tree leaf maximum in this case. The wind speed of 0.80 m s^{-1} at the top level of Tower 2 was smaller than the speed in Case 1, while the wind within the canopy at Tower 2 ranged from 0.12 m s^{-1} in the trunk space to 0.30 m s^{-1} at the top of the canopy. At the second level of Tower 2 (5 m in height), where near-zero carbon dioxide flux and heat flux were measured, we note a wind speed of 0.19 m s^{-1} from the northeast. Although the air is in motion at this height, the vertical turbulent fluxes for carbon dioxide, sensible heat, and latent heat (Figure 6j) were minimal during this time period.

The Obukhov stability parameter (Figure 6g) indicated unstable atmosphere at the bottom of Tower 2, while the rest of Tower 2 and the top of Tower 1 were stable. In this case, the Obukhov stability parameter did not give reasonable predictions of atmospheric stability.

3.3. Case 3—Stable Atmosphere

At 1 A.M. on 30 May 2013, the vertical potential temperature profile at Tower 1 had cold air at the base of the tower, with potential temperature increasing slightly (but steadily) with altitude. Tower 2 also recorded increasing potential temperature with height (Figure 8a), indicating a stable atmosphere. The wind directions were westerly at the lower levels of both towers. The top of Tower 1 recorded wind from the southwest, while the top of Tower 2 experienced southeasterly wind. As in Case 2, wind roses provide an additional visual indication of wind direction and its variability to mitigate possible inaccuracies in average wind direction during periods of low wind speed (Figures 9a–9f). Air flowed north to south at the top of the canopy at Tower 2 (level 2–4), possibly indicating tridimensional flow [*Tóta et al.*, 2012], with air deflecting horizontally around the hill obstructing the background flow, though with only two towers we could not expand our investigation to three dimensions. The vertical velocity at level 2–4 during this time period was −0.067 m s^{-1}, indicating very little vertical motion. No vertical recirculation pattern was visible (Figure 6b). The wind rose for the top of the

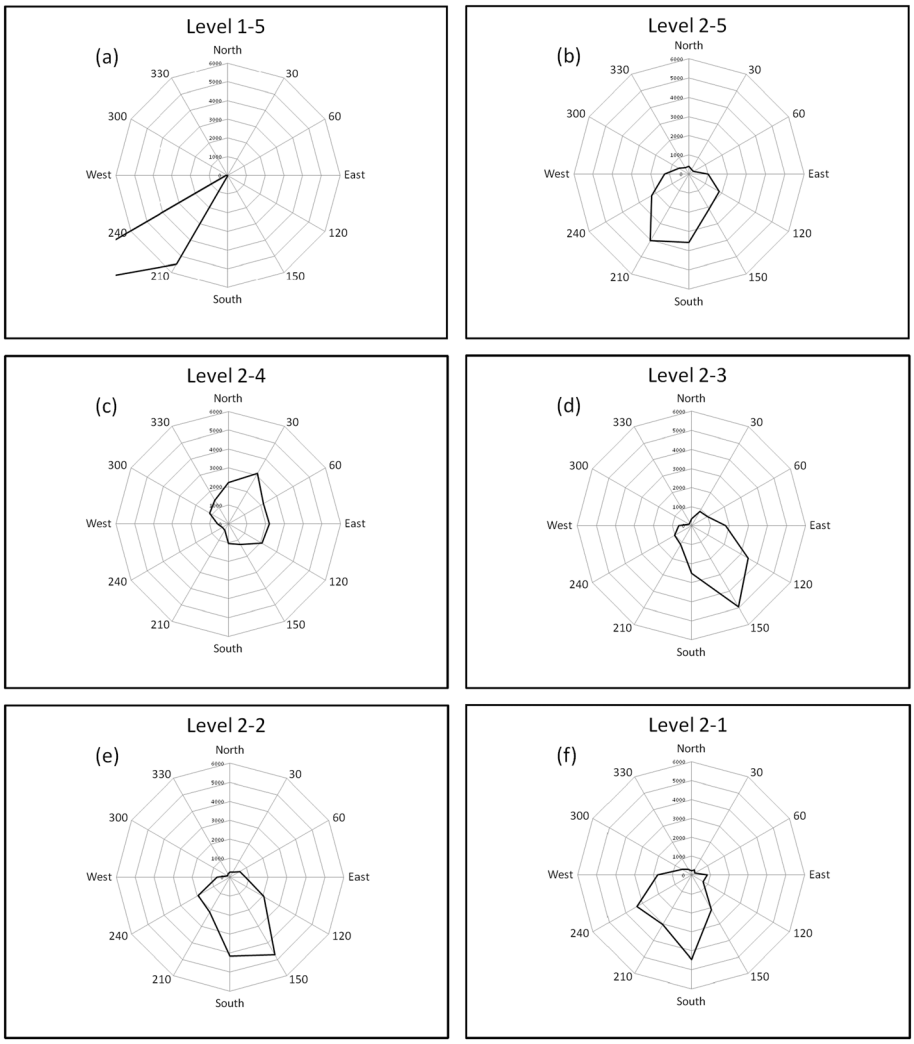

Figure 9. Wind roses (in degrees) at 1:00 A.M. on 30 May 2013, showing (a) top of Tower 1, (b) top of Tower 2, (c) top of canopy at Tower 2, (d) midcanopy at Tower 2, (e) lower canopy at Tower 2, and (f) trunk space at Tower 2. The wind roses were assembled using counts of the unrotated wind direction collected at 10 Hz over 30 min and are not weighted by wind speed.

canopy at Tower 2 (Figure 9c) indicates airflow from the north, northeast, east, and southeast. The near-zero vertical velocity at level 2–4, combined with the wind direction and wind rose, reinforces the supposition that the air flow wrapped around the hillside horizontally rather than displacing vertically. A conceptual sketch of the two-dimensional hillside air dynamics for Case 3 is included as Figure 5c.

Under stable atmospheric conditions where potential temperature increases with height (causing a decrease in density with height), lee waves may be caused by the pressure drop as the air mass passes over the hilltop [*Wurtele et al*., 1993]. With our experimental setup, we were unable to confirm the theorized lee waves during the experiment. However, during this time period, the Brunt-Väisälä equation determined a period of about 186 s for a standing atmospheric wave at the top of Tower 2, which informed our conceptual sketch (Figure 5c). A spectral analysis of vertical wind speed fluctuations during this time period did not show an obvious peak at any frequency. Speculatively, lee waves could possibly have occurred at an elevation near the top of the canopy on the hilltop, approximately 15 m above the height of Tower 2's topmost sensor suite and therefore beyond the reach of this project setup.

Lower in the canopy near Tower 2, katabatic flow was observed as the dense cold air mass close to the ground, rich in carbon dioxide, flowed slowly down the hill. Carbon dioxide concentration on the slope was poorly mixed (Figure 8c), indicating a stratified atmosphere with no effective vertical mixing. If the

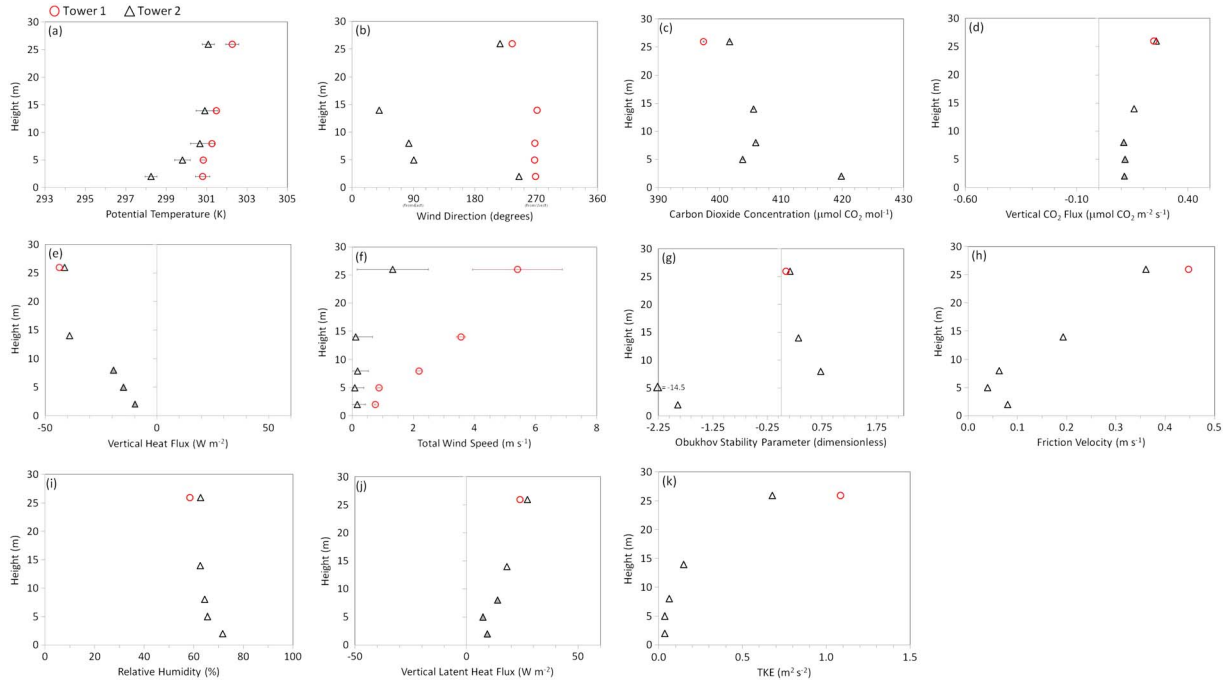

Figure 10. Charts of the observation results at 11:00 P.M. on 30 May 2013, showing (a) potential temperature, (b) wind direction, (c) carbon dioxide concentration, (d) carbon dioxide flux, (e) heat flux, and (f) total wind speed. Tower 1 results are represented by red circles, while Tower 2 data are black triangles. Gray triangles indicate fluxes with $u_* < 0.17$ m s^{-1}. Charts of the observation results at 11:00 P.M. on 30 May 2013, showing (g) Obukhov stability parameter, (h) friction velocity, (i) relative humidity, (j) vertical latent heat flux, and (k) turbulent kinetic energy. Tower 1 results are represented by red circles, while Tower 2 data are black triangles. Gray triangles indicate fluxes with $u_* < 0.17$ m s^{-1}.

atmosphere around Tower 2 had been well mixed by a recirculation zone, the carbon dioxide concentration measured at the top of Tower 2 would be higher. Tower 2 showed little or no carbon dioxide flux, while energy flux was generally downward except at level 2–3 (Figures 8d and 8e). The total wind speeds recorded (Figure 8f) showed increasing speed with height at Tower 1, reaching a maximum at the top of the canopy and decreasing slightly with additional height. As in Case 1, the wind at Tower 2 was at a minimum in midcanopy, showing the influence of trees on the air flow [*Yi*, 2008]. The top level wind speed of 0.51 m s^{-1} was larger than the speed in the trunk space, 0.21 m s^{-1}. The large relative difference between the Tower 2 top level wind speed and the bottom level (nearly 60%) contrasts with the difference recorded in Case 1 (just over 30%), further supporting the evidence that the lower levels experienced a different air mass with distinct dynamics that would not be uncovered by sampling only the top level at Tower 2, despite the acceptable 0.21 m s^{-1} friction velocity (Figure 8h).

3.4. The Inconvenient Case

Our theory failed to predict the atmospheric dynamics during one evening in the middle of the project. At 11 P.M. on 30 May 2013, 22 h after Case 3 above, a partial recirculation eddy was measured (Figure 10b). Wind roses provide an additional visual indication of wind direction and its variability to mitigate possible inaccuracies in average wind direction during periods of low wind speed (Figures 11a–11f). At that time, the vertical potential temperature profile indicated stable atmospheric conditions (Figure 10a). The stability began at least 3 h prior, between 7 P.M. and 8 P.M. As the stability strengthened toward midnight, the eddy dissipated for the rest of the night. The vertical profiles show a partially mixed carbon dioxide concentration (Figure 10c), upward carbon dioxide flux (Figure 10d), and downward heat flux (Figure 10e). The total wind speeds recorded increasing speed with height at Tower 1 (Figure 10f). Wind speeds at Tower 2 were very low at all four lower levels, with faster wind at the top level.

A peculiarity during this time period can be seen in the wind rose for the top of the canopy (Figure 11c). Compared with the same level in Case 2's partial recirculation profile, this time period's level 2–4 reversed flow contains a significant but nondominant amount of streamwise flow. This oscillating flow may indicate

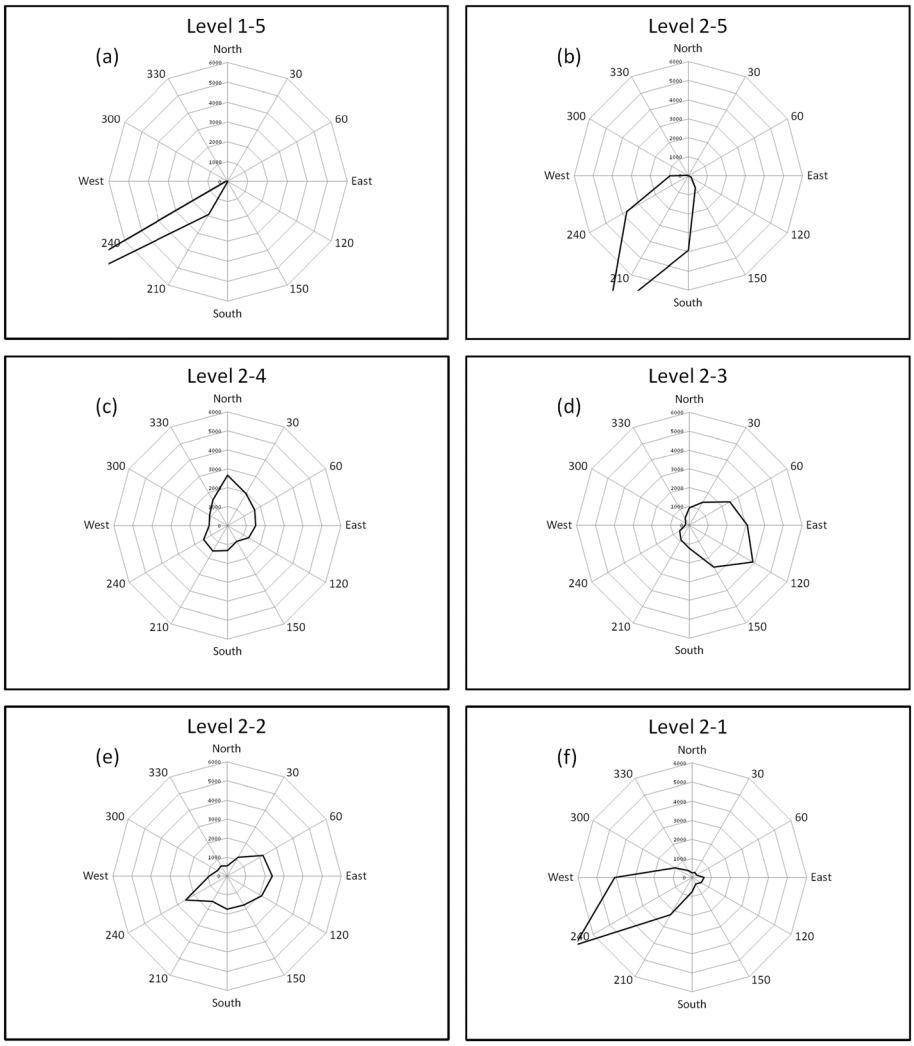

Figure 11. Wind roses (in degrees) at 11:00 P.M. on 30 May 2013, showing (a) top of Tower 1, (b) top of Tower 2, (c) top of canopy at Tower 2, (d) midcanopy at Tower 2, (e) lower canopy at Tower 2, and (f) trunk space at Tower 2. The wind roses were assembled using counts of the unrotated wind direction collected at 10 Hz over 30 min and are not weighted by wind speed.

measurement of the wake effect caused by a single treetop near the tower, which the background wind coincidentally aimed at the sensor during this time period. This anomaly could also have been caused by stronger winds, at 5.4 m s^{-1} (Tower 1, top level), compared with 3.8 m s^{-1} for Case 3. Strong winds may cause stratification of the boundary layer, with a small eddy downwind of an obstruction [*Stull*, 1988], which coincidentally may have been located at Tower 2 at the time in question. Also, while simulations [e.g., *Xu et al*., 2015] show that recirculation eddies may be caused over complex terrain without a background wind, a large pressure drop in the lee of the obstruction caused by strong winds might briefly cause recirculation despite the stable atmosphere, simply due to the angular momentum of the wind parcel. We note that the Brunt-Väisälä equation for this time period predicted a lee wave with a period of about 283 s, which is a significantly longer waveform than Case 3.

4. Concluding Remarks

To determine atmospheric stability, we used potential temperature instead of Obukhov's stability parameter. In almost all cases, the vertical gradient of the potential temperature determined the type of atmospheric circulation pattern observed in the lee of the hill. Whenever the vertical potential temperature gradient indicated unstable conditions and the site experienced westerly winds, Tower 2 recorded recirculation. Under

stable conditions, there was no evidence of recirculation at Tower 2, except for one time period mentioned in section 3.4 above. Transitions and hybrid conditions (such as the partial recirculation noted in Figures 5b and 6b) occurred during near-neutral situations.

The full recirculation condition discussed as Case 1 was surprising in that it reached the forest floor despite a positive vertical potential temperature gradient between the bottommost two levels. During those time periods with full recirculation, the colder, denser air from the forest floor at Tower 2 flowed uphill, rising into the warmer, less dense air aloft. The mechanically induced recirculation flow was strong enough to drive countergradient air flow.

Since recirculating air does not conform to the assumption of zero flow divergence or convergence required in eddy covariance calculations, we urge additional caution when using eddy flux tower data taken over complex terrain during time periods of thermally unstable atmospheric conditions. The use of carbon dioxide eddy flux calculations from such time periods for net ecosystem exchange analyses may not be accurate regardless of friction velocity. We recommend additional multitower studies to determine modifications to the eddy covariance method in situations where divergence or convergence occurs.

Aubinet [2008] remarked that gravity waves (or lee waves) could cause noise in eddy flux measurements and undermine stationarity or similarity assumptions required for a complete application of the eddy covariance method. During time periods where the vertical potential temperature gradient resulted in stable conditions, our conceptual formulation of the atmospheric dynamics took the form of a standing wave locked to the hill and valley topography. While the standing wave could not be confirmed using this two-tower system, either positive or negative vertical carbon dioxide fluxes were measured on separate evenings with similar potential temperatures and potential temperature gradients. The Brunt-Väisälä equation describes the frequency of such a standing wave as a function of the vertical potential temperature gradient and the temperature itself. The wavelength will vary depending on frequency and also wind speed. An additional variable to consider is the distance between the obstruction that causes the lee wave and the tower recording a part of the phenomenon (in this case Tower 2). The vertical direction of the measured flux will depend on the frequency (i.e., the potential temperature and the vertical potential temperature gradient), the wind speed, and the distance between the obstruction and the recording instruments. All other parameters being roughly equivalent on two separate averaging periods, one wind speed may result in a positive vertical carbon dioxide flux and another results in a negative flux, simply because of the point in the standing wave's oscillation at which the slope tower's sensors are situated.

Acknowledgments

This project was supported by National Science Foundation (NSF) grant 0930015, and City University of New York, PSC-CUNY ENHC-68849-00 46. Liu's participation in the field work was supported by NSF Atmospheric and Geospace Sciences (AGS) under grant 1419614. Special thanks to Qianyu Zhang of Washington State University for crucial assistance with our installing, maintaining, and dismantling of the two towers and to Black Rock Forest Consortium for their much-needed guidance and help. Deep appreciation also goes to the numerous City University of New York students, faculty, and staff from Queens College, City College and Hunter College who spent many hours in a forest working hard in pursuit of science. The base data are available upon request from Chuixiang Yi (cyi@qc.cuny.edu). We are also grateful to three anonymous reviewers for their insightful comments and constructive criticisms that have improved our manuscript.

References

Aubinet, M. (2008), Eddy covariance CO_2 flux measurements in nocturnal conditions: An analysis of the problem, *Ecol. Appl.*, *18*(6), 1368–1378.

Baldocchi, D. (2003), Assessing the eddy covariance technique for evaluating carbon dioxide exchange rates of ecosystems: Past, present and future, *Glob. Chang. Biol.*, *9*, 1–14.

Baldocchi, D., B. Hincks, and T. Meyers (1988), Measuring biosphere-atmosphere exchanges of biologically related gases with micrometeorological methods, *Ecology*, *69-5*, 1331–1340.

Budyko, M. (1958), *The Heat Balance of the Earth's Surface*, p. 259 , *U.S. Department of Commerce*, Washington, D. C.

Burba, G., and D. Anderson (2010), *A Brief Practical Guide to Eddy Covariance Flux Measurements*, Li-Cor Biosciences, Nebr.

Chen, H., and C. Yi (2012), Optimal control of katabatic flows within canopies, *Q. J. R. Meteorol. Soc.*, *138*, 1676–1680, doi:10.1002/qj.1904.

Dawson, P., S. David, and B. Lamb (1991), The numerical simulation of airflow and dispersion in three-dimensional atmospheric recirculation zones, *J. Appl. Meteorol.*, *31*, 1005–1024.

Feigenwinter, C., L. Montagnani, and M. Aubinet (2010), Plot-scale vertical and horizontal transport of CO_2 modified by a persistent slope wind system in and above an alpine forest, *Agric. For. Meteorol.*, *150*, 665–673.

Finnigan, J., and S. E. Belcher (2004), Flow over a hill covered with a plant canopy, *Q. J. R. Meteorol. Soc.*, *130*, 1–29.

Finnigan, J. (2008), An introduction to flux measurements in difficult conditions, *Ecol. Appl.*, *18*(6), 1340–1350.

Foken, T. (2006), 50 years of the Monin-Obukhov similarity theory, *Boundary Layer Meteorol.*, *119*, 431–447.

Foken, T. (2008), The energy balance closure problem: An overview, *Ecol. Appl.*, *18*(6), 1351–1367.

Goulden, M., J. Munger, S. Fan, B. Daube, and S. Wofsy (1996), Measurements of carbon sequestration by long-term eddy covariance: Methods and a critical evaluation of accuracy, *Glob. Chang. Biol.*, *2*, 169–182.

Gu, J., E. Smith, and J. Merritt (1999), Testing energy balance closure with GOES-retrieved net radiation and in situ measured eddy correlation fluxes in BOREAS, *J. Geophys. Res.*, *104*(D22), 27,881–27,893, doi:10.1029/1999JD900390.

Kaimal, J. C., and L. Kristensen (1991), Time series tapering for short data samples, *Boundary Layer Meteorol.*, *57*, 187–194.

Katul, G. G., J. Finnigan, D. Poggi, R. Leuning, and S. E. Belcher (2006), The influence of hilly terrain on canopy–atmosphere carbon dioxide exchange, *Boundary Layer Meteorol.*, *118*, 189–216, doi:10.1007/s10546-005-6436-2.

Kljun, N., P. Calanca, M. W. Rotach, and H. P. Schmid (2004), A simple parameterisation for flux footprint predictions, *Boundary Layer Meteorol.*, *112*, 503–523.

Mauder, M., and T. Foken (2004), Documentation and instruction manual of the Eddy covariance software package TK2, Arbeitsergebnisse Nr. 26.

Moncrieff, J. B., J. M. Massheder, H. de Bruin, J. Ebers, T. Friborg, B. Heuskinveld, P. Kabat, S. Scott, H. Soegaard, and A. Verhoef (1997), A system to measure surface fluxes of momentum, sensible heat, Water vapor and carbon dioxide, *J. Hydrol.*, *188–189*, 589–611.

Moncrieff, J. B., R. Clement, J. Finnigan, and T. Meyers (2004), Averaging, detrending and filtering eddy covariance time series, in *Handbook of Micrometeorology: A Guide for Surface Flux Measurements*, edited by X. Lee, W. J. Massman, and B. E. Law, pp. 7–31, Kluwer Acad., Dordrecht, Netherlands.

Monin, A. S., and A. M. Obukhov (1954), Basic laws of turbulent mixing in the surface layer of the atmosphere, *Tr. Akad. Nauk. SSSR Geophiz. Inst.*, *24*(151), 163–187.

Papale, D., and R. Valentini (2003), A new assessment of European forests' carbon exchanges by eddy fluxes and artificial neural network spatialization, *Glob. Chang. Biol.*, *9*, 525–535.

Poggi, D., and G. G. Katul (2007), Turbulent flows on forested hilly terrain: The recirculation region, *Q. J. R. Meteorol. Soc.*, *133*, 1027–1039.

Raupach, M. R., and A. S. Thom (1981), Turbulence in and above plant canopies, *Annu. Rev. Fluid Mech.*, *13*, 97–129.

Staebler, R., and D. Fitzjarrald (2005), Measuring canopy structure and the kinematics of subcanopy flows in two forests, *J. Appl. Meteorol.*, *44*, 1161–1179.

Stull, R. B. (1988), *An Introduction to Boundary Layer Meteorology*, pp. 601–609, Kluwer Acad., Dordrecht, Netherlands.

Tóta, J., D. Fitzjarrald, R. Staebler, R. Sakai, O. Moraes, O. Acevedo, S. Wofsy, and A. Manzi (2008), Amazon rain forest subcanopy flow and the carbon budget: Santarém LBA-ECO site, *J. Geophys. Res.*, *113*, G00B02, doi:10.1029/2007JG000597.

Tóta, J., D. Fitzjarrald, and M. da Silva Dias (2012), Amazon rainforest exchange of carbon and subcanopy air flow: Manaus LBA site—A complex terrain condition, *Sci. World J.*, 19, doi:10.1100/2012/165067.

Vickers, D., and L. Mahrt (1997), Quality control and flux sampling problems for tower and aircraft data, *J. Atmos. Ocean. Technol.*, *14*, 512–526.

Wang, W., and C. Yi (2012), A new nonlinear analytical model for canopy flow over a forested hill, *Theor. Appl. Climatol.*, doi:10.1007/s00704-012-0599-9.

Webb, E., G. Pearman, and R. Leuning (1980), Correction of flux measurement for density effects due to heat and water vapour Transfer, *Q. J. R. Meteorol. Soc.*, *106*, 85–100.

Whiteman, C. D. (2000), *Mountain Meteorology: Fundamentals and Applications*, pp. 144–151, Oxford Univ. Press, New York.

Wilczak, J. M., S. P. Oncley, and S. A. Stage (2001), Sonic anemometer tilt correction algorithms, *Boundary Layer Meteorol.*, *99*, 127–150.

Wilson, K., et al. (2002), Energy balance closure at FLUXNET sites, *Agric. For. Meteorol.*, *113*, 223–243.

Wurtele, M. G., A. Datta, and R. D. Sharman (1993), Lee waves: Benign and malignant, NASA Contractor Report 186024, Dryden Flight Research Facility, Edwards, Calif.

Xu, X., and C. Yi (2012), The influence of geometry on recirculation and CO_2 transport over forested hills, *Meteorog. Atmos. Phys.*, doi:10.1007/s00703-012-0224-6.

Xu, X., C. Yi, and E. Kutter (2015), Stably stratified canopy flow in complex terrain, *Atmos. Chem. Phys.*, *15*(13), 7457–7470.

Xu, X., C. Yi, L. Montagnani, and E. Kutter (2017), Numerical study of the interplay between thermo-topographic slope flow and synoptic flow on canopy transport processes, *Agric. For. Meteorol.*, doi:10.1016/j.agrformet.2017.03.004.

Yi, C., R. Monson, Z. Zhai, D. Anderson, B. Lamb, G. Allwine, A. Turnipseed, and S. Burns (2005), Modeling and measuring the nocturnal drainage flow in a high-elevation, subalpine forest with complex terrain, *J. Geophys. Res.*, *110*, D22303, doi:10.1029/2005JD006282.

Yi, C. (2008), Momentum transfer within canopies, *J. Appl. Meteorol. Climatol.*, *47*, 262–275, doi:10.1175/2007JAMC1667.1.